SI

A general acetic acid vapour etching strategy to synthesize layered carbon nitride with carbon vacancies for efficient photoredox catalysis

Jianghong Zhao[1*], Rihui Mu[1], Ya Zhang[2], Zhidong Yang[2], Hongxia Zhang[2], Hu Shi[2,3*], Min Zhang[2], Zhanfeng Zheng[4], and Pengju Yang[2,4*]

[1]Engineering Research Center of Ministry of Education for Fine Chemicals, Shanxi University, Taiyuan 030006, China

[2]School of Chemistry and Chemical Engineering, Shanxi University, Taiyuan 030006, China

[3]Institute of Molecular Science, Shanxi University, Taiyuan 030006, China

[4]State Key Laboratory of Coal Conversion, Institute of Coal Chemistry, Chinese Academy of Sciences, Taiyuan 030001, China

Contents:

of PCN-T and PCN-T nanosheets.

Figure S25. Mott−Schottky plots of (a) PCN-D and (b) PCN-D nanosheets. (c) Band alignments of PCN-D and PCN-D nanosheets.

Figure S26. Comparison of the degradation rates of PCN-T and PCN-T nanosheets.

Figure S27. Comparison of the degradation rates of PCN-D and PCN-D nanosheets.

Table S1. The BET data of all samples.

Table S2. The atom percentage of C, N and O atoms in the PCN and PCN nanosheets samples determined by XPS.

Table S3. The peaks area ratios of C-N=C/H-N=C, N-$(C)_3$ and C-NHx of PCN and PCN nanosheets.

Table S4. The atom percentage of C, N, O and H atoms in the PCN and PCN nanosheets samples determined by EA.

Table S5. Comparison of typical PCN photocatalysts reported for hydrogen production and the corresponding quantum yields.

Table S6. Bader charge analysis located in the Pt/PCN interface. The value was obtained by the difference between the number of valence electrons and calculated Bader charge results for each atom. The positive and negative values stand for, respectively, electron loss and accumulation. The net electronic charges transferred from the PCN to the Pt are -0.296 |e|.

Table S7. Bader charge analysis located in the Pt/PCN-CVs interface. The value was obtained by the difference between the number of valence electrons and calculated Bader charge results for each atom. The positive and negative values stand for, respectively, electron loss and accumulation. The net electronic charges transferred from the PCN-CVs to the Pt are -0.44 |e|.

Table S8. Free energy corrections for various reaction species

Table S9. Bader charge transfer of atoms located in the O_2/PCN interface. The value was obtained by the difference between the number of valence electrons and calculated Bader charge results for each atom. The net electronic charges transferred from the PCN interface to the O_2 are -2.01 |e|.

Table S10. Bader charge transfer of atoms located in the O_2/PCN-CVs interface. The value was obtained by the difference between the number of valence electrons and calculated Bader charge results for each atom. The net electronic charges transferred from the PCN nanosheets interface to the O_2 are -2.476 |e|.

Table S11. The atom percentage of C, N and O atoms in the PCN-T, PCN-T nanosheets, PCN-D

and PCN-D nanosheets samples determined by XPS.

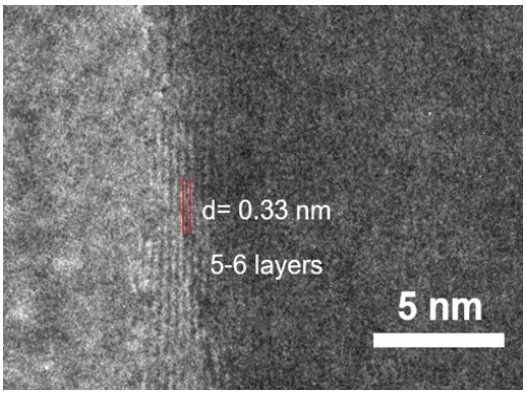

Figure S1. Result of the edge layer number of PCN nanosheets by TEM analysis.

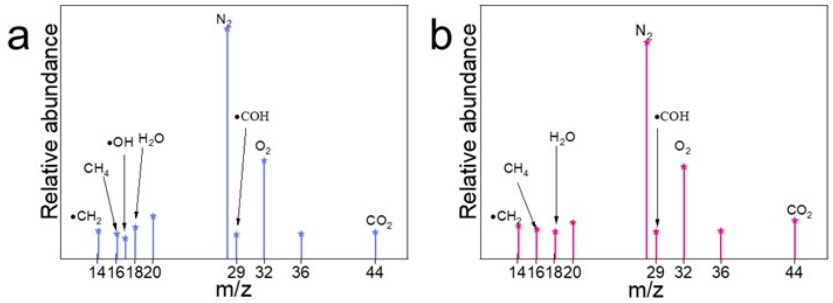

Figure S2. Mass spectrometry analysis of acetic acid decomposition (a) and acetic acid decomposition in presence of PCN (b).

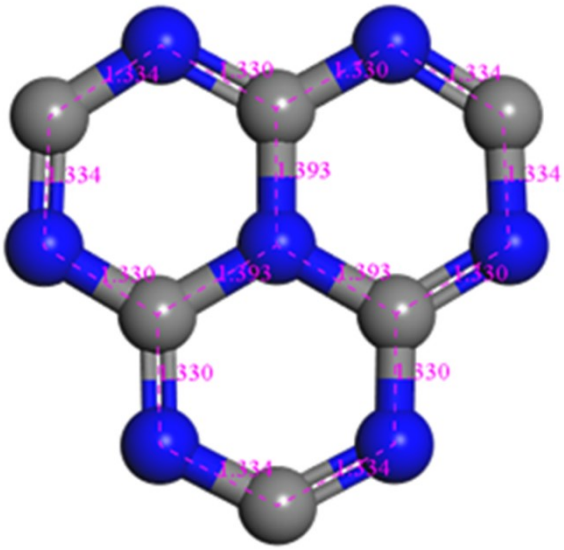

Figure S3. The bond lengths of C/N and C=N bonds within PCN.

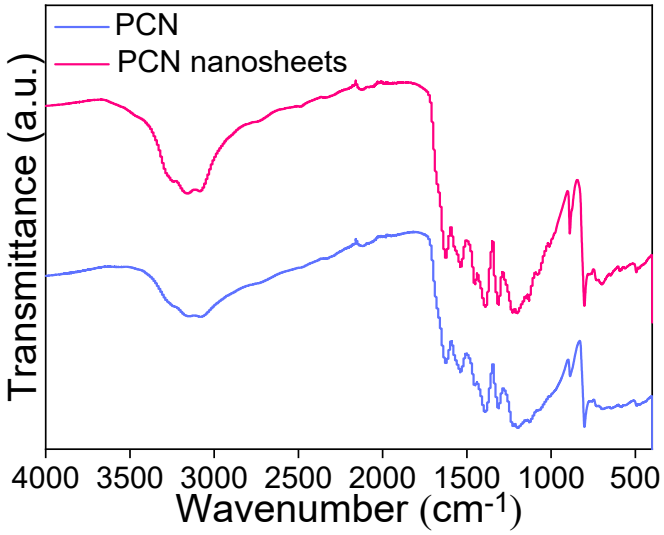

Figure S4. FTIR spectra of PCN and PCN nanosheets.

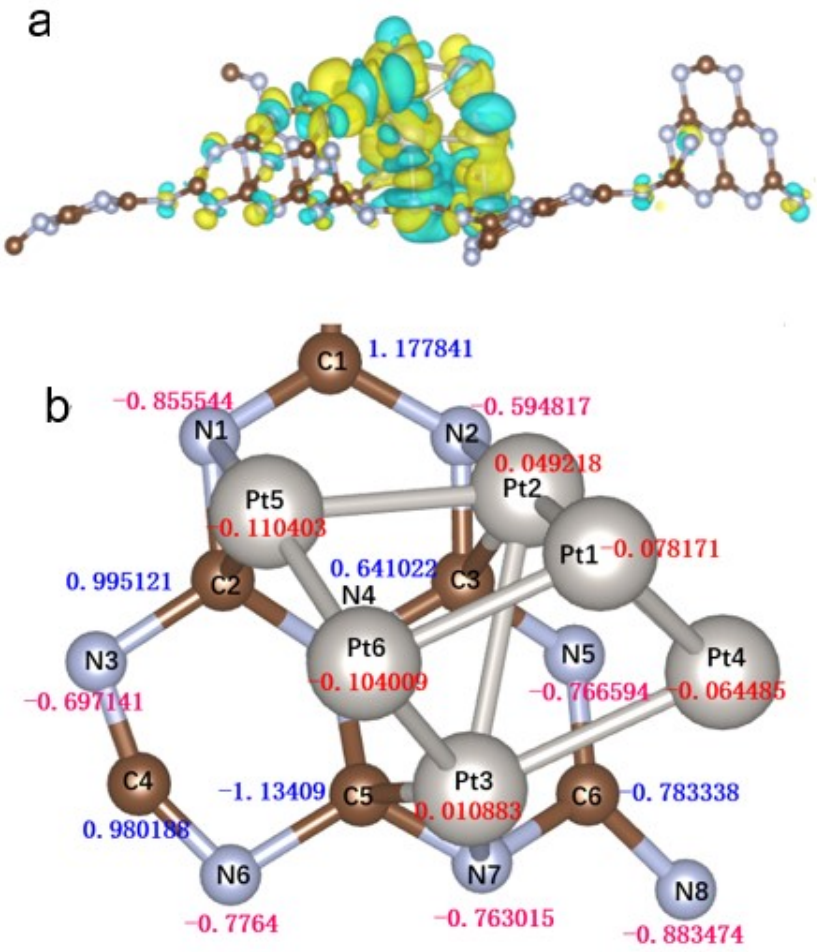

Figure S5. (a) Charge density difference and (b) Bader charge analysis of Pt/PCN. The cyan and yellow indicate the regions of charge loss and gain, respectively.

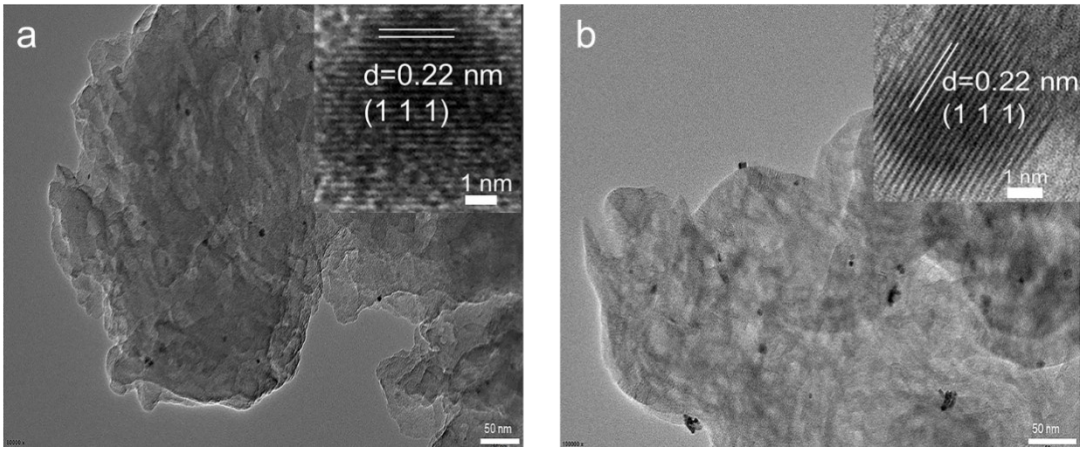

Figure S6. TEM images of Pt/PCN (a) and Pt/PCN nanosheets (b) (inset is the HRTEM images of Pt nanoparticles).

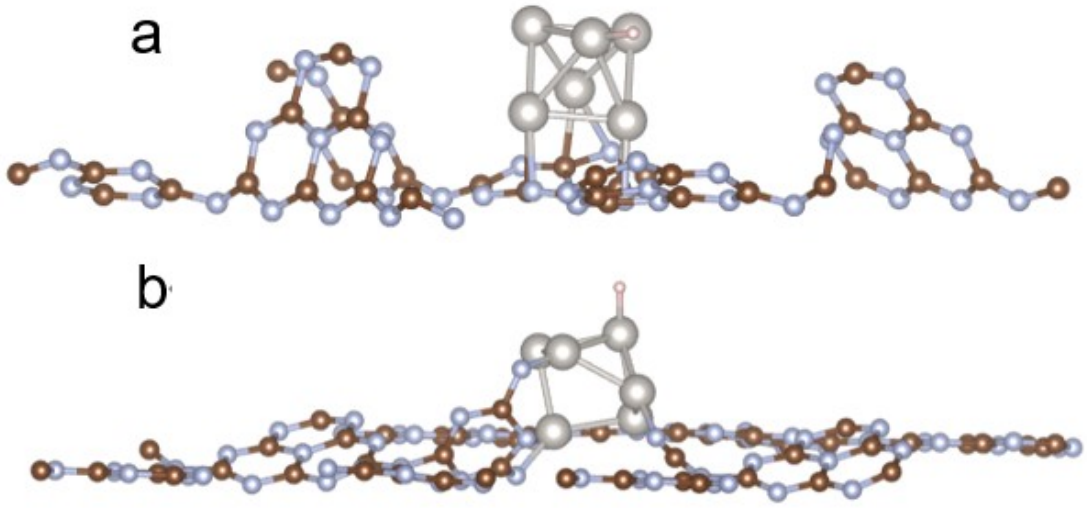

Figure S7. Optimized geometric structures of (a) Pt/PCN-H*, (b) Pt/PCN-CVs-H* by DFT simulation.

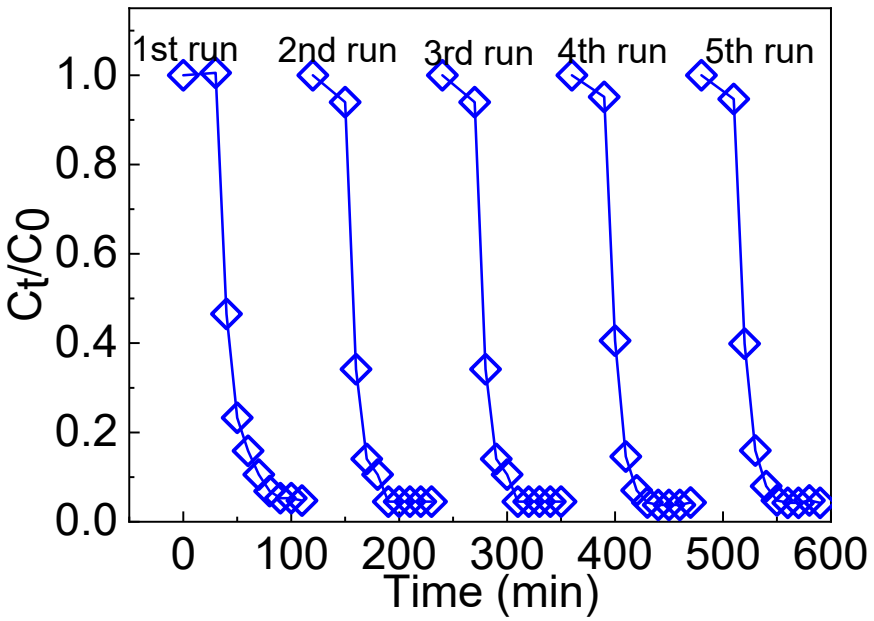

Figure S8. Cycling experiments of PCN nanosheets toward phenol degradation.

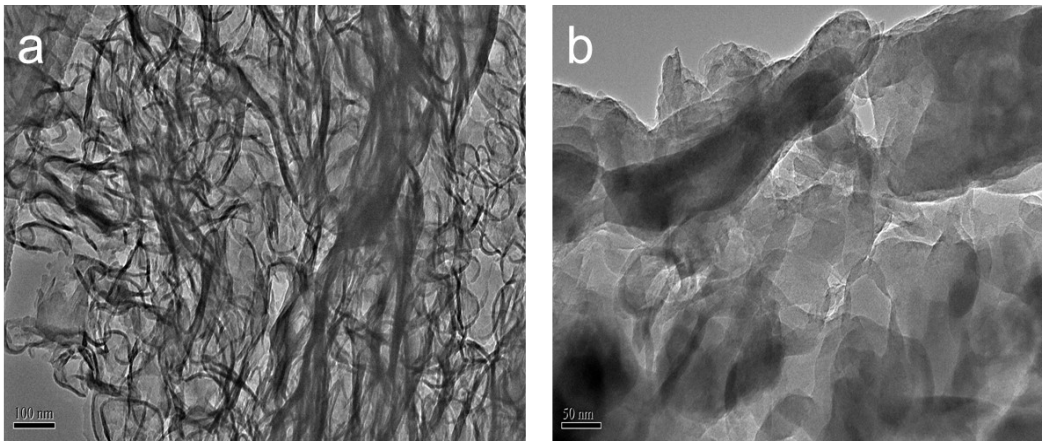

Figure S9. TEM images of PCN-T and PCN-D.

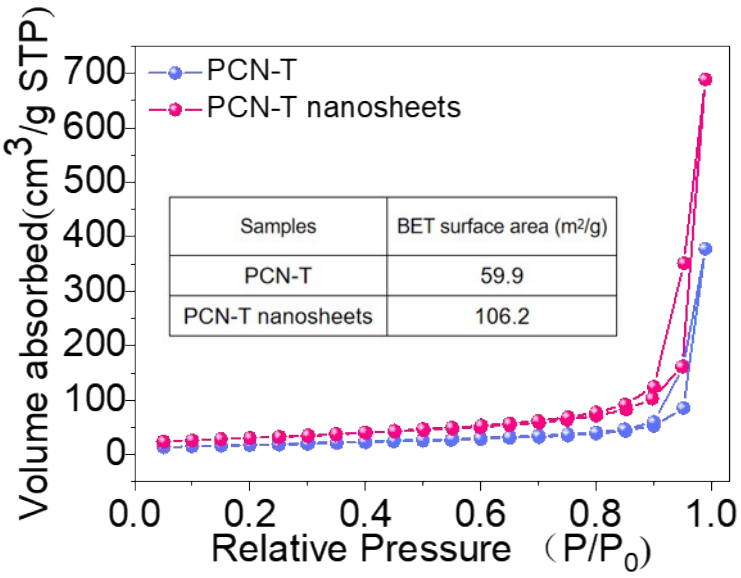

Figure S10. Nitrogen adsorption−desorption isotherms of PCN-T and PCN-T nanosheets.

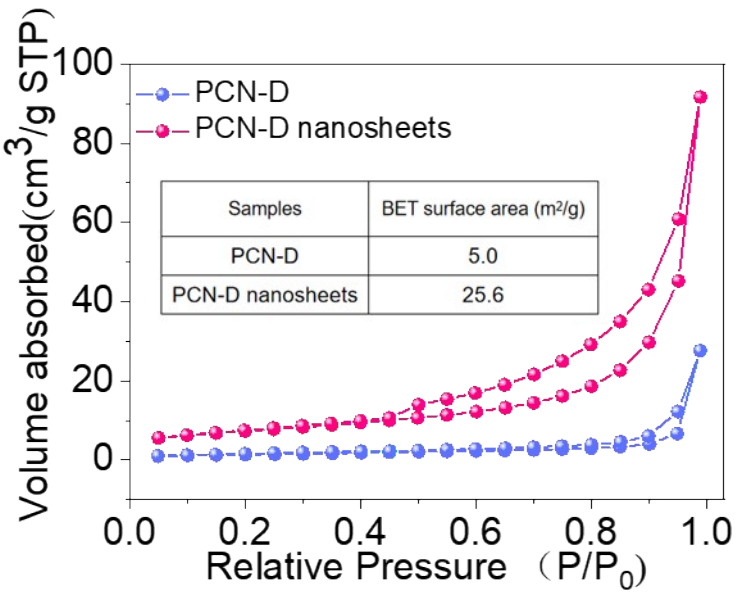

Figure S11. Nitrogen adsorption−desorption isotherms of PCN-D and PCN-D nanosheets.

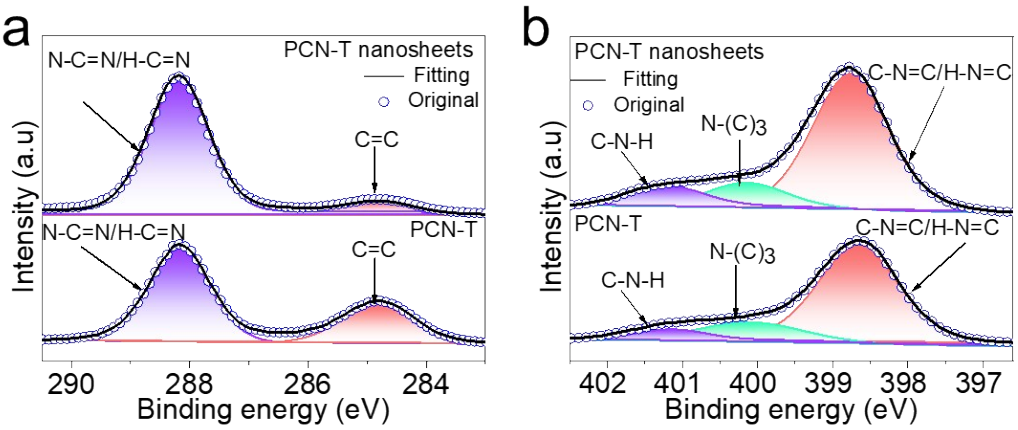

Figure S12. (a) C 1s and (b) N 1s of PCN-T and PCN-T nanosheets.

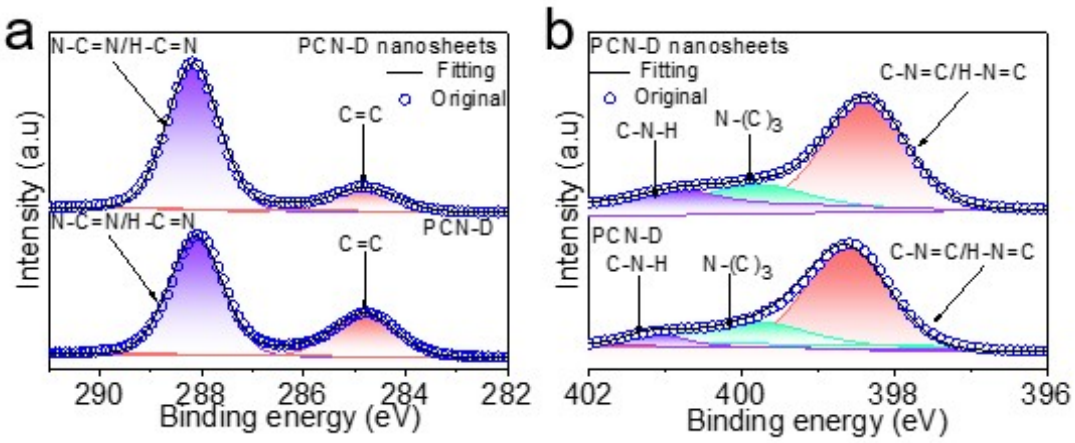

Figure S13. (a) C 1s and (b) N 1s of PCN-D and PCN-D nanosheets.

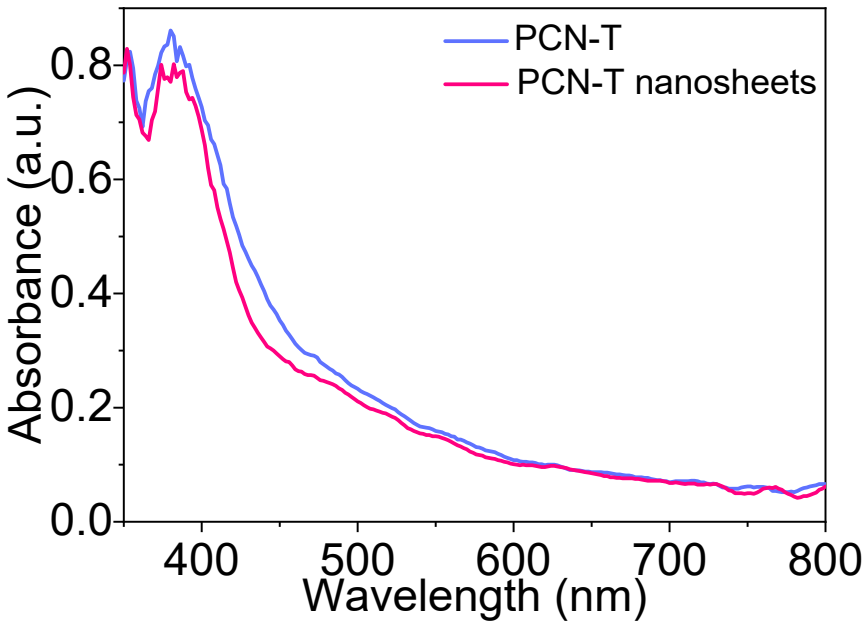

Figure S14. UV−vis spectra of PCN-T and PCN-T nanosheets.

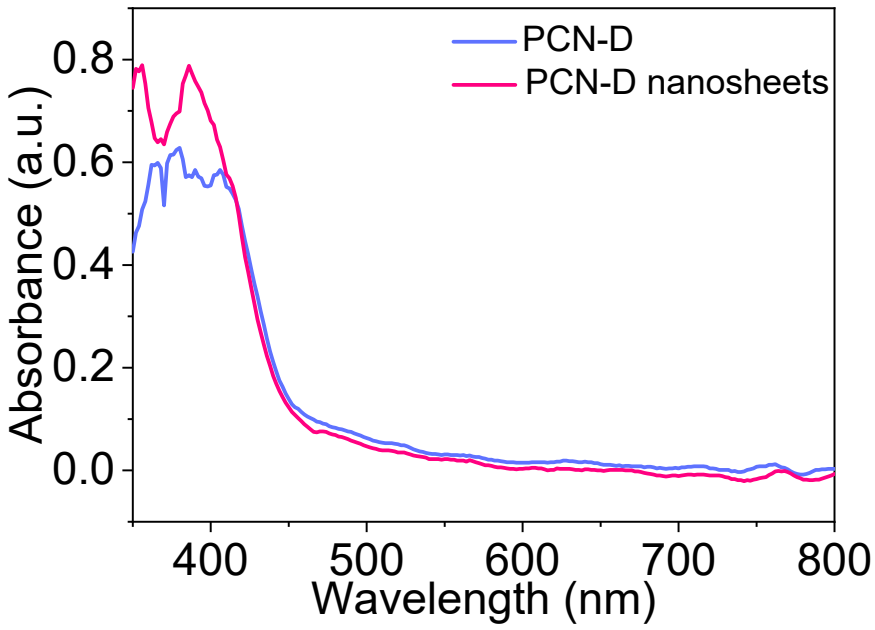

Figure S15. UV−vis spectra of PCN-D and PCN-D nanosheets.

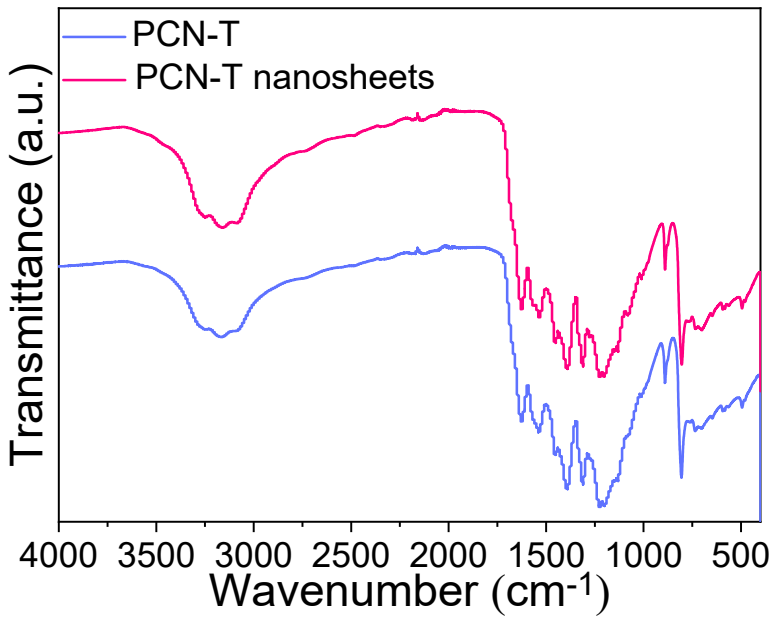

Figure S16. FTIR spectra of PCN-T and PCN-T nanosheets.

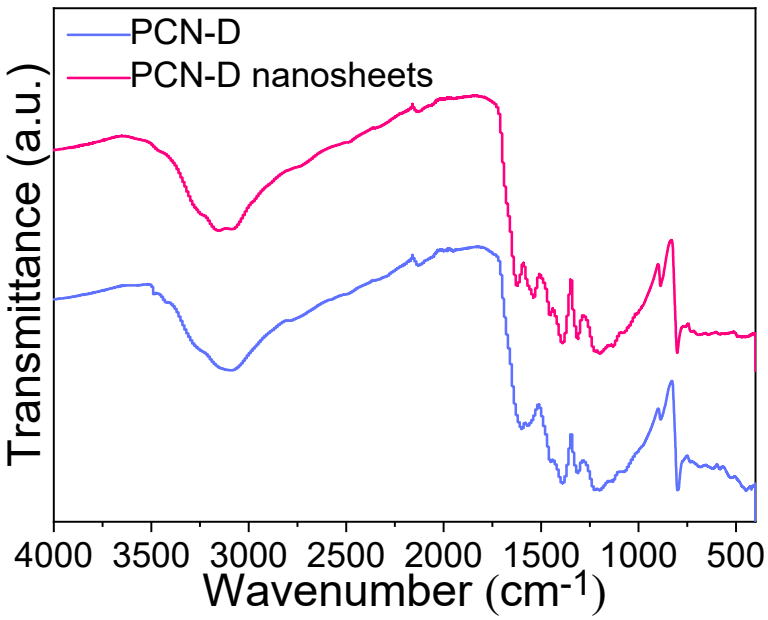

Figure S17. FTIR spectra of PCN-D and PCN-D nanosheets.

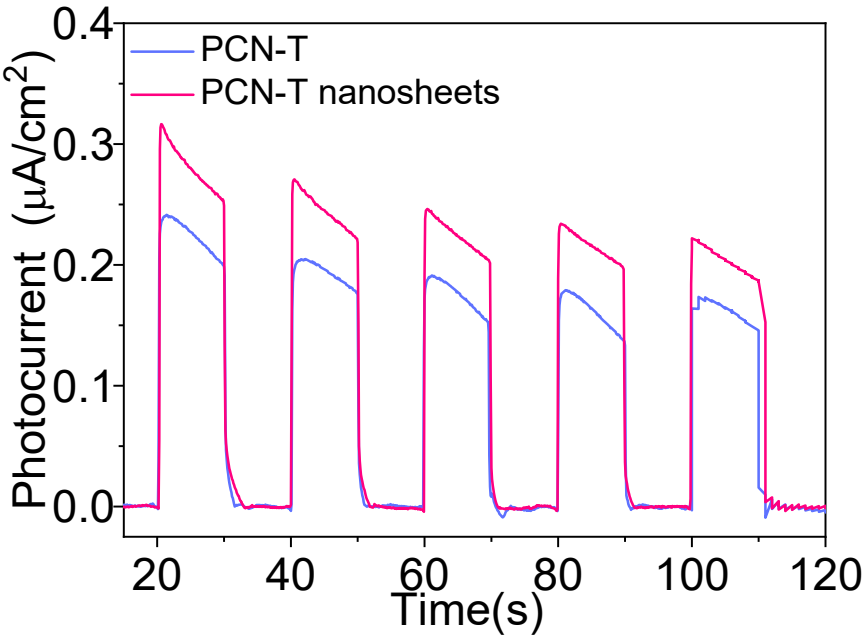

Figure S18. Transient photocurrent density of PCN-T and PCN-T nanosheets under 420 nm.

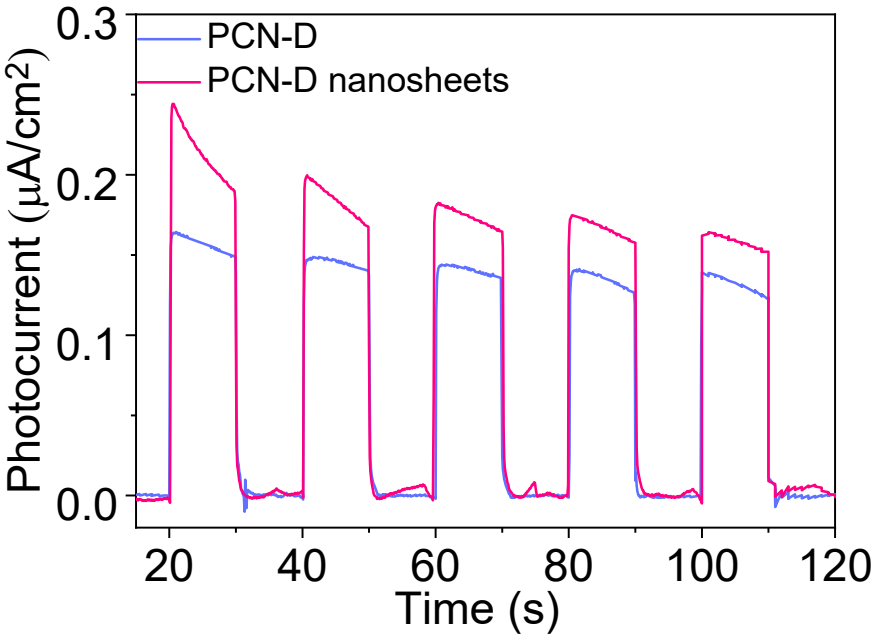

Figure S19. Transient photocurrent density PCN-D and PCN-D nanosheets under 420 nm.

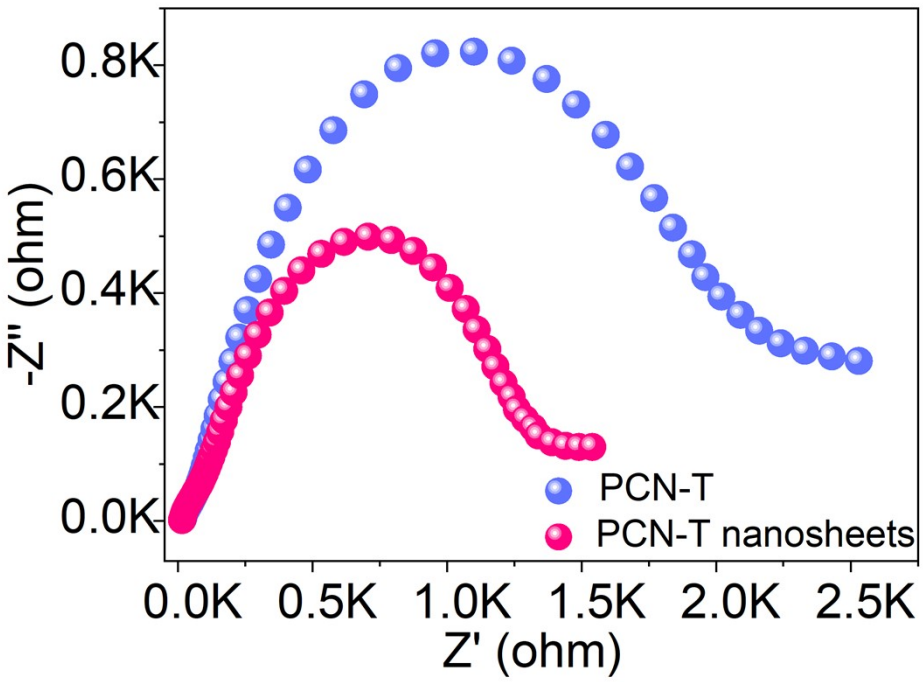

Figure S20. Electrochemical impedance spectra of PCN-T and PCN-T nanosheets.

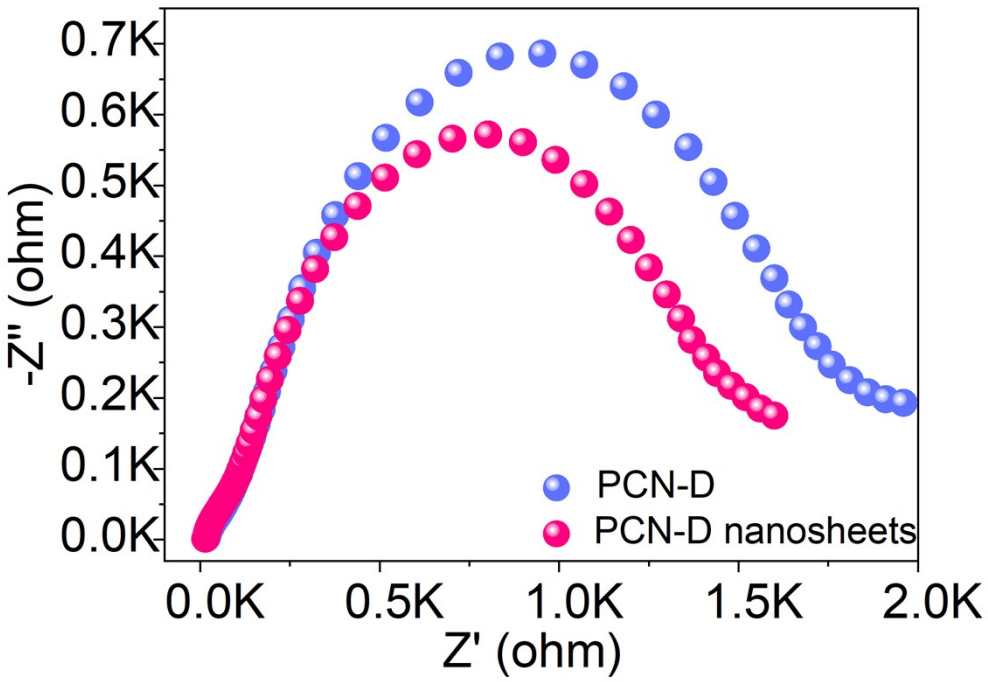

Figure S21. Electrochemical impedance spectra of PCN-D and PCN-D nanosheets.

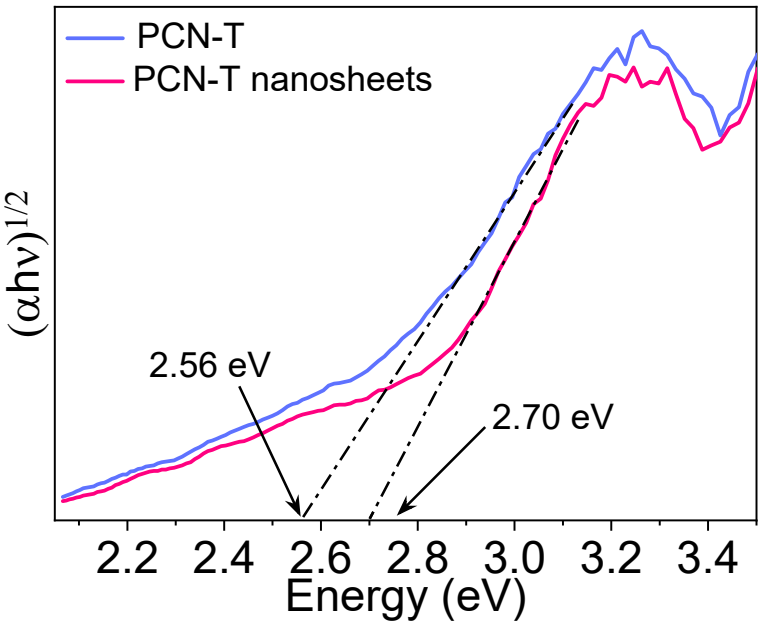

Figure S22. Band gap energies of PCN-T and PCN-T nanosheets.

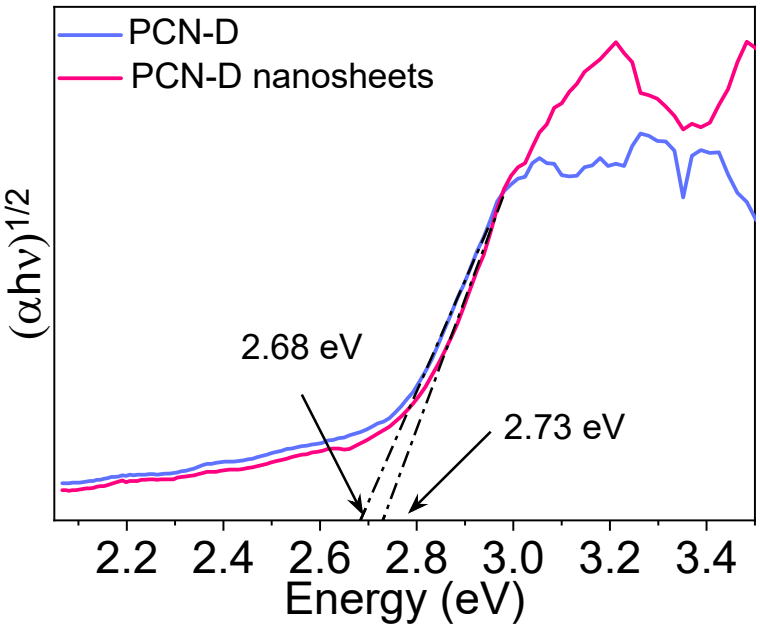

Figure S23. Band gap energies of PCN-D and PCN-D nanosheets.

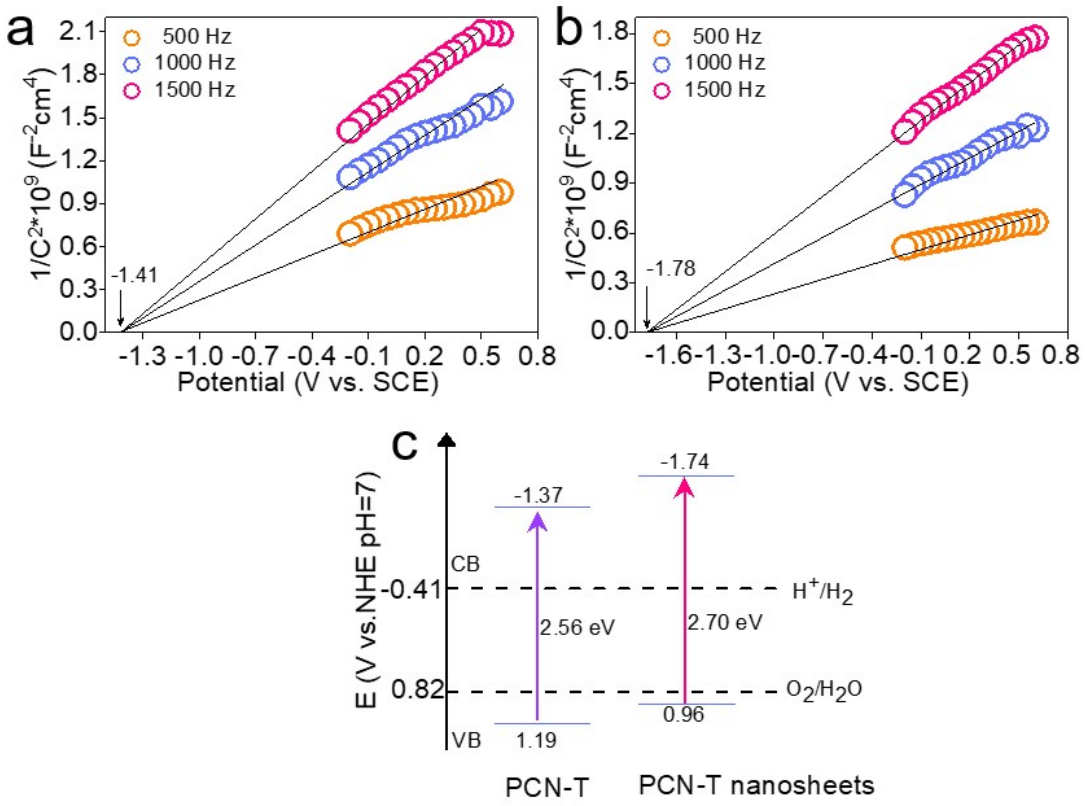

Figure S24. Mott−Schottky plots of (a) PCN-T and (b) PCN-T nanosheets. (c) Band alignments of PCN-T and PCN-T nanosheets.

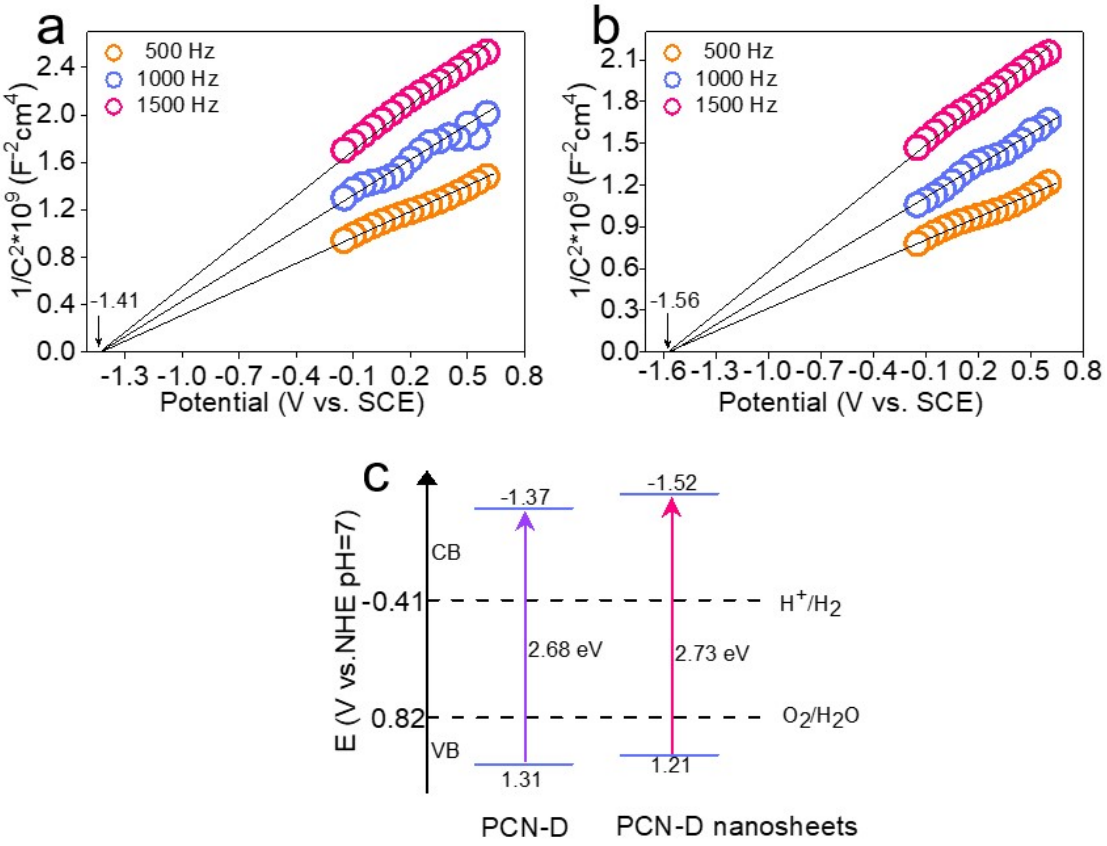

Figure S25. Mott−Schottky plots of (a) PCN-D and (b) PCN-D nanosheets. (c) Band alignments of PCN-D and PCN-D nanosheets.

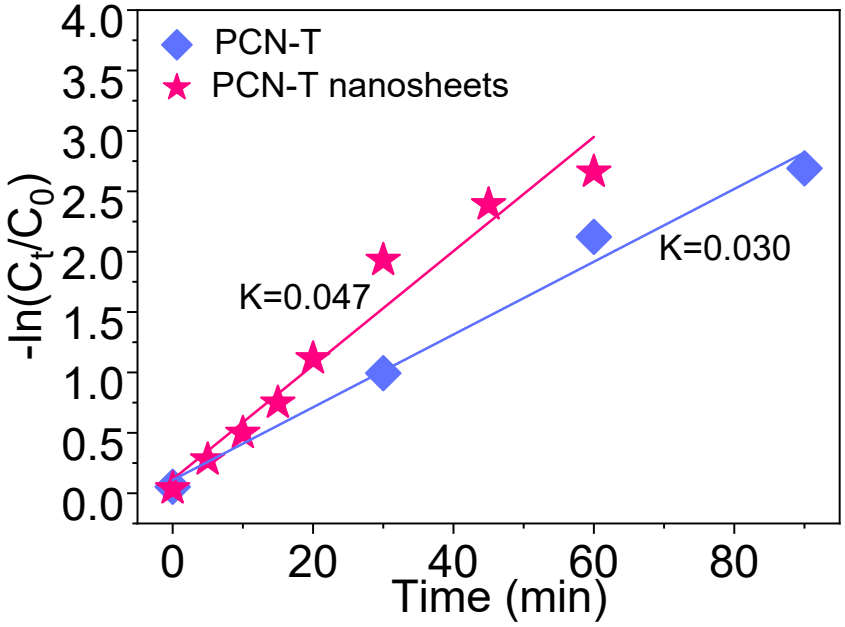

Figure S26. Comparison of the degradation rates of PCN-T and PCN-T nanosheets.

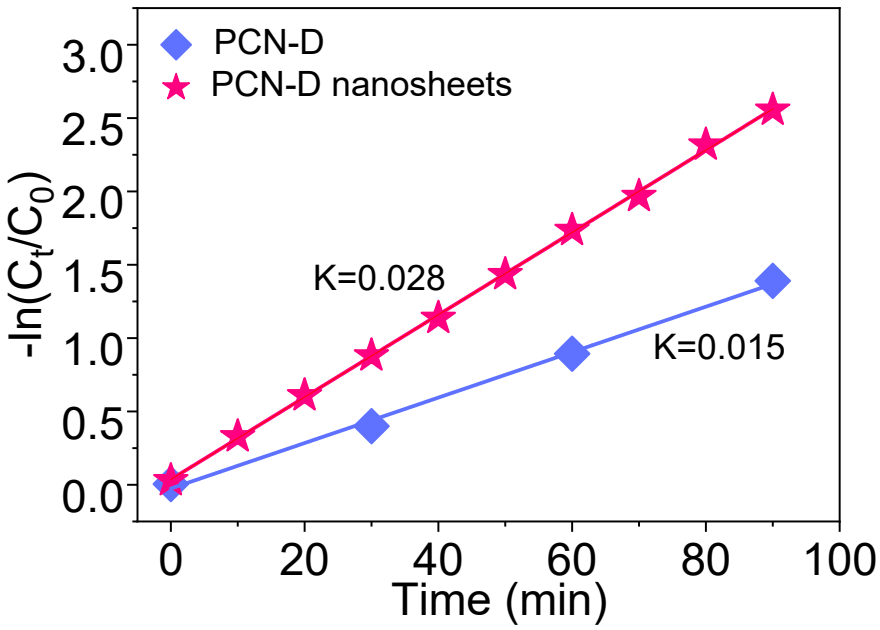

Figure S27. Comparison of the degradation rates of PCN-D and PCN-D nanosheets.

Table S1. The BET data of all samples.

Samples	BET surface areas (m^2/g)
PCN	8.6
PCN nanosheets	177.0
PCN-T	59.9
PCN-T nanosheets	106.2
PCN-D	5.0
PCN-D nanosheets	25.6

Table S2. The atom percentage of C, N and O atoms in the PCN and PCN nanosheets samples determined by XPS.

Samples	C (at%)	N (at%)	O (at%)	C/N (at%)
PCN	45.94	50.18	3.88	0.916
PCN nanosheets	42.96	53.68	3.36	0.800

Table S3. The peaks area ratios of C-N=C/H-N=C, N-$(C)_3$ and C-NHx of PCN and PCN nanosheets.

Samples	C-N=C/H-N=C (%)	N-C_3 (%)	C-NH_X (%)
PCN	75.2	15.6	9.2
PCN nanosheets	76.2	13.5	10.3

Table S4. The atom percentage of C, N, O and H atoms in the PCN and PCN nanosheets samples determined by EA.

Samples	C (at%)	N (at%)	O (at%)	H (at%)	C/N (at%)
PCN	30.3	46.0	4.3	19.4	0.659
PCN nanosheets	29.5	44.9	3.9	21.7	0.657

Table S5. Comparison of typical PCN photocatalysts reported for hydrogen production and the corresponding quantum yields.

Photocatalyst	light source(nm)	HER rate (μmol/g/h)	AQY%	Ref.
PCN nanosheets	50w LED light (400nm)		16.22 (400nm)	**This work**
	50w LED light (420nm)	4020	7.96 (420nm)	**This work**
PCN-T nanosheets	50w LED light (400nm)		28.77 (400nm)	**This work**
	50w LED light (420nm)	11010	21.38 (420nm)	**This work**
PyP2/CN	300 W Xe lamp ($\lambda \geq 420$ nm)	600	3.75 (420nm)	1
COC30	300 W Xe lamp ($\lambda \geq 420$ nm)	1336	8.41 (420 nm)	2
CN-10	300 W Xe lamp ($\lambda \geq 400$ nm)	459	2.2 (420 nm)	3
p-CN2	300 W Xe lamp ($\lambda > 420$ nm)	396	0.79 (420 nm)	4
CN-UNS	300 W Xe lamp ($\lambda \geq 420$ nm)	5740	14.49 (420 nm)	5
DTLP-CN	500 W Xe lamp ($\lambda \geq 420$ nm)	1557	11.2 (420 nm)	6
GCN	300 W Xe lamp(AM 1.5 filter)	9904	10.3 (380 nm)	7
HCN-NEA	300 W Xenon lamp ($\lambda \geq 420$ nm)	4092	7.87 (420nm)	8
3CuL/PCN	300 W Xenon lamp ($\lambda > 420$ nm)	795	2.49 (420 nm)	9
D-CCN	monochromatic LED lamps	1280	2.50 (405 nm) 3.40 (420 nm) 5.70 (450 nm)	10
m-PCN_1	monochromatic LED lamps	604	1.10 (405 nm) 0.75 (420 nm) 0.22 (450 nm)	11
m-CNNS	monochromatic LED lamps	2600	8.10 (420 nm)	12
CN aerogels	monochromatic LED lamps	600	3.10 (420 nm)	13
PCN-U nanosheets	monochromatic LED lamps	3390	11.3 (405 nm)	14

Table S6. Bader charge analysis located in the Pt/PCN interface. The value was obtained by the difference between the number of valence electrons and calculated Bader charge results for each atom. The positive and negative values stand for, respectively, electron loss and accumulation. The net electronic charges transferred from the PCN to the Pt are -0.296 |e|.

Atoms	1	2	3	4	5	6	7	8
C	1.1778	0.9951	0.6410	0.9802	-1.1340	-0.7833		
N	-0.8555	-0.5948	-0.6971	0.6410	-0.7666	-0.7764	-0.7630	-0.8835
Pt	-0.0782	0.0492	0.0109	-0.0645	-0.1104	-0.1040		

Table S7. Bader charge analysis located in the Pt/PCN-CVs interface. The value was obtained by the difference between the number of valence electrons and calculated Bader charge results for each atom. The positive and negative values stand for, respectively, electron loss and accumulation. The net electronic charges transferred from the PCN-CVs to the Pt are -0.44 |e|.

Atoms	1	2	3	4	5	6
C	1.2402	1.0256	0.7402	0.9481		
N	-0.4820	-0.7137	-0.9387	-0.4673	-0.9902	-0.3754
Pt	0.1538	0.0427	0.0337	-0.2941	-0.1757	-0.2006

Table S8. Free energy corrections for various reaction species.

Species	E_{DFT} (eV)	E_{ZPE} (eV)	∫CpdT(eV)	-TS (eV)	G (eV)
Pt/PCN	-490.67	0.00	0.09	0.00	-490.67
Pt/PCN-H*	-491.99	0.19	0.10	-0.03	-491.83
PCN-CVs	-485.62	0.00	0.09	0.00	-485.62
Pt/PCN-CVs-H*	-490.35	0.19	0.10	-0.02	-490.18

Table S9. Bader charge transfer of atoms located in the O_2/PCN interface. The value was obtained by the difference between the number of valence electrons and calculated Bader charge results for each atom. The net electronic charges transferred from the PCN interface to the O_2 are -2.01 |e|.

Atoms	1	2	3	4	5	6
N	-0.772	-0.899	-0.833	-0.714	-0.895	-0.677
C	2.087	2.047	1.961	2.139	1.910	-2.015
O	-1.041	-0.969				

Table S10. Bader charge transfer of atoms located in the O_2/PCN-CVs interface. The value was obtained by the difference between the number of valence electrons and calculated Bader charge results for each atom. The net electronic charges transferred from the PCN-CVs interface to the O_2 are -2.476 |e|.

Atoms	1	2	3	4	5	6	7	8	9
N	-0.752	-0.116	-0.731	-0.632	-0.527	-0.879	-0.822	-0.863	-0.602
C	2.271	1.959	1.992	2.249	1.864				
O	-1.157	-1.320							

Table S11. The atom percentage of C, N and O atoms in the PCN-T, PCN-T nanosheets, PCN-D and PCN-D nanosheets samples determined by XPS.

Samples	C (at%)	N (at%)	O (at%)	C/N (at%)
PCN-T	49.19	46.42	4.40	1.06
PCN-T nanosheets	42.63	55.66	1.71	0.77
PCN-D	48.11	47.79	4.11	1.01
PCN-D nanosheets	43.25	53.78	2.97	0.80

References:

1. S. Zang, G. Zhang, P. Yang, D. Zheng and X. Wang, *Chem. Eur. J.,* 2019, 25, 6102-6107.
2. C. Yang, Z. Xue, J. Qin, M. Sawangphruk, X. Zhang and R. Liu, *Appl. Catal. B Environ.,* 2019, 259, 118094.
3. F. Yang, D. Liu, Y. Li, L. Cheng and J. Ye, *Appl. Catal. B Environ.,* 2019, 240, 64-71.
4. Y. Jiang, Z. Sun, C. Tang, Y. Zhou, L. Zeng and L. Huang, *Appl. Catal. B Environ.*, 2019, 240, 30-38.
5. Y. Zhang, Z. Huang, C.-L. Dong, J. Shi, C. Cheng, X. Guan, S. Zong, B. Luo, Z. Cheng, D. Wei, Y.-c. Huang, S. Shen and L. Guo, *Chem. Eng. J.,* 2022, 431, 134101.
6. Y. Huang, J. Liu, C. Zhao, X. Jia, M. Ma, Y. Qian, C. Yang, K. Liu, F. Tan, Z. Wang, X. Li, S. Qu and Z. Wang, *ACS Appl Mater Interfaces*, 2020, 12, 52603-52614.
7. W. Jiang, Y. Zhao, X. Zong, H. Nie, L. Niu, L. An, D. Qu, X. Wang, Z. Kang and Z. Sun, *Angew. Chem. Int. Ed.*, 2021, 60, 6124-6129.
8. Q. Liu, F. Wang, Y. Jiang, W. Chen, R. Zou, J. Ma, L. Zhong and X. Peng, *Carbon*, 2020, 170, 199-212.
9. Y. Zhang, Q. Cao, X. Wu, Y. Xiao, A. Meng, Q. Zhang, Y. Yu and W.-D. Zhang, *Chem. Eur. J.,* 2022, 427, 132042.
10. W. Ren, J. Cheng, H. Ou, C. Huang, M. M. Titirici and X. Wang, *ChemSusChem*, 2019, 12, 3257-3262.
11. L. Yin, S. Wang, C. Yang, S. Lyu and X. Wang, *ChemSusChem*, 2019, 12, 3320-3325.
12. H. Ou, C. Tang, Y. Zhang, A. M. Asiri, M.-M. Titirici and X. Wang, *J. Catal.*, 2019, 375, 104-112.
13. H. Ou, P. Yang, L. Lin, M. Anpo and X. Wang, *Angew. Chem. Int. Ed.*, 2017, 56, 10905-10910.
14. P. Yang, H. Ou, Y. Fang and X. Wang, *Angew. Chem. Int. Ed.*, 2017, 56, 3992-3996.